International Journal of Pressure Vessels and Piping 144 (2016) 1–10

Contents lists available at ScienceDirect

International Journal of Pressure Vessels and Piping

journal homepage: www.elsevier.com/locate/ijpvp

Residual stress characterization of single and triple-pass autogenously welded stainless steel pipes

R.D. Haigh [a], M.T. Hutchings [a], M.E. Fitzpatrick [a, f, *], J.A. James [a], S. Okido [b], R. Mizuno [c], K. Ogawa [c], D.J. Hughes [d, e]

[a] Materials Engineering, The Open University, Walton Hall, Milton Keynes, MK7 6AA, UK
[b] Material, Strength and Reliability Unit, Department of Material Research for Power Plants, Hitachi Research Laboratory, Hitachi, Ltd. 3-1-1, Saiwai-cho, Hitachi-shi, Ibaraki, 317-8511, Japan
[c] Nondestructive Evaluation Center, Japan Power Engineering and Inspection Corporation, 14-1, Benten-cho, Tsurumi-ku, Yokohama, 230-0044, Japan
[d] Institut Laue-Langevin, 6 Rue Jules Horowitz, BP 156, Grenoble Cedex, F-38042, France
[e] WMG, International Digital Laboratory, University of Warwick, Coventry, CV4 7AL, UK
[f] Faculty of Engineering and Computing, Coventry University, Priory Street, Coventry, CV1 5FB, UK

ARTICLE INFO

Article history:
Received 10 July 2014
Received in revised form
19 May 2016
Accepted 22 May 2016
Available online 24 May 2016

Keywords:
Autogenous welds
Residual stress
Neutron diffraction

ABSTRACT

Using neutron diffraction the components of the residual stress field have been determined in the region near a mid-length groove in two identical austenitic stainless pipes in which weld beads had been laid down. One pipe sample had a single pass, and the second a triple pass, autogenous weld deposited around the groove circumference. The results show the effect on the stress field of the additional weld deposited and are compared to the results of Finite Element Modelling. The hoop stress component is found to be generally tensile, and greater in the triple pass weldment than in the single pass weldment. The hoop stresses reach peak values of around 400 MPa in tension. X-ray measurements of the residual stress components on the near inner surface of the pipe weldments are also presented, and show tensile stresses in both pipes, with a higher magnitude in the three-pass weldment.

1. Introduction

The primary area of component cracking in power plant piping is in welded joints. One of the main causes of failure in welded pipes is stress corrosion cracking (SCC), and the likelihood of this occurring is highly-dependent on residual stresses present in the weld region. Prediction of the magnitude and profile of the residual stress distribution in coolant pipe work is extremely difficult, and experimental validation of finite element-based models of residual stress generation is required [1–4]. The work described here is part of a programme aimed at understanding the residual stress built up in circumferential weldments in austenitic steel pipes.

Neutron diffraction techniques are a powerful means for non-destructive in-depth determination of residual stresses [5]. By fabrication of plant-scale mock-ups using controlled fabrication conditions, experimental samples can be provided in which the fabrication history is well-defined. Measurement of such samples can provide knowledge of the residual stresses arising from thermal histories during welding. During the cool down and solidification following a weld pass deposition, molten material will shrink and tend to pull all other material with it. In the case of butt-welded pipe weldments this manifests itself as a circumferential contraction about the girth weld. The parent metal near to the heat-affected zone (HAZ) will partially resist the deformation, and it is this partial resistance or partial flow which results in residual stresses. After welding, tensile residual stresses usually develop in both the weld metal and the heat-affected zone (HAZ) metal. The magnitude of the residual stress field is affected by the pipe's diameter, its thickness, and the size of the weld bead. Girth weld beads generally lead to high tensile residual stresses on the inside surface of the pipe [1]. In particular it is tensile residual stresses in the HAZ which contribute to SCC. Successive weld passes, in a multi-weld pass weld, will result in a cyclic accumulation of both residual elastic stresses and plastic strains.

This work is aimed at determining how stresses develop as the number of weld passes increases. By comparison with predictions from Finite Element Modelling (FEM) the neutron diffraction

* Corresponding author. Faculty of Engineering and Computing, Coventry University, Priory Street, Coventry, CV1 5FB, UK.
E-mail address: michael.fitzpatrick@coventry.ac.uk (M.E. Fitzpatrick).

http://dx.doi.org/10.1016/j.ijpvp.2016.05.003
0308-0161/

results will help validate FEM analysis of the change in stress profile in welded pipes on filling the weld. The results of near-inner surface measurements using X-ray diffraction are also presented.

There has been much work done in the last two decades on comparison between measured and modeled residual stresses in welded components [10,11]. This has led to improvements in both experimental and modelling approaches to the determination of weld residual stress. However, the geometries studied have generally been relatively simple, such as a bead-on-plate or bead-in-groove specimen [12]. In this study, we have looked at a more complex geometry, with the intention of understanding the residual stress generation in autogenous welds. The modelling is used to provide support to the experimental data. This complements the wider body of work on the determination of residual stress in materials and components for nuclear power and similar applications [13–20].

In complementary work related to that presented here, neutron diffraction has been used to measure the residual stress distribution throughout the weld area in two specially fabricated multi-pass girth-welded austenitic stainless steel pipes of similar dimensions to those discussed here. However in that case the weldments were formed by joining two half-length sections of pipe, where one weldment had weld metal deposited in the joining groove up to half the pipe wall thickness, and one with weld metal deposited up to full pipe wall thickness [6].

2. Sample weldments

2.1. Manufacture

The two samples examined were fabricated from a length of austenitic stainless steel pipe, type 304. The starting material was a 3500 mm length of pipe of outer diameter 318.5 mm and inner diameter 251.9 mm. This was cut and ground to make two pipes of length 500 mm with outer diameter 305 mm and inner diameter 255 mm. These sample pipes were then subjected to solution annealing in vacuum, with a heating rate of <200 °C per hour, a hold temperature of 900 °C ± 5 °C for 2 h, followed by cooling at a rate of <275 °C per hour.

A groove was then cut to a depth of half the wall thickness around the mid-length diameter, with dimensions shown in Fig. 1. Weld beads were then laid down in the flat position inside the groove by automatic TIG welding (GTAW). The welding current was 132 A, voltage 10 V, and speed 9 cm/min. There was no pre-heating. The inter-pass temperature was <150 °C. The composition of the parent pipe metal and the weld metal is given in Table 1.

2.2. The co-ordinate system

It was necessary to carefully establish a sample coordinate system for each weldment in order to define the measurement

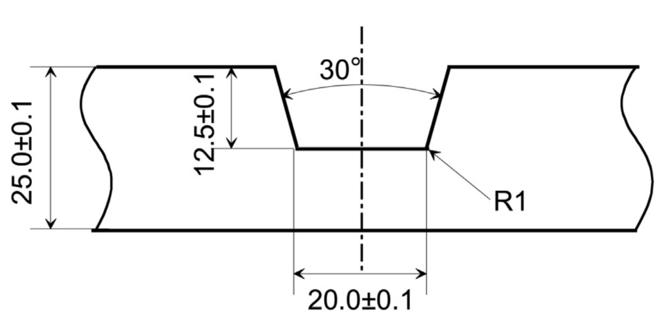

Fig. 1. The dimensions in mm of the groove cut at the mid axis point of the pipes.

Table 1
The chemical composition of the austenitic stainless steel pipe, type 304.

	Composition/wt %							
	C	Si	Mn	P	S	Ni	Cr	Fe
Pipe (Parent) Metal	0.010	0.42	1.49	0.019	n.d.	9.15	18.19	70.72

positions. This is shown in Fig. 2. Here x, y, z are Cartesian axes with origin at the centre of the weldment. The x axis is along the axial direction of the pipe, and the z axis along a radial direction defined by the azimuthal angle $\alpha = 0$. Measurement angles and radii were denoted as α and r respectively as shown in Fig 2(iii). The azimuthal angles α were engraved on each weldment in steps of 90°. It should be noted that α is taken as positive in the clockwise direction when looking along the axial negative x direction, with zero angle along the +z axis. The shape of the pipe weldment lends itself to a cylindrical coordinate system, which is here expressed as r, α, x. A reference point denoted **T**, top dead centre (TDC), was located in these cylindrical coordinates at (139.07, 0, 250), and in the Cartesian coordinates at (250, 0, 139.07), as shown in Figs. 2 and 3. An access slot aperture was machined at the 90° position with its centre at Cartesian coordinates (0, 140, 0) in order to facilitate access by the neutron beam through minimising absorption losses of beam intensity. It is assumed that this slot will not affect the stress distribution as it is distanced from the measurement positions.

Both pipes were circumferentially welded autogenously around the central groove. The weld was laid down in the increasing α direction, with the first and third pass start and stop positions being at the $\alpha = 0°$ position, and the second pass start and stop positions being at $\alpha = 180°$. For each weld pass the moving heat source was briefly paused at the position 180° from start. The dimensions of the single-pass pipe weldment and the position of the weld pass with respect to the x axis are shown in Fig. 3a, the centre of the single pass weld is at x = +6.6 mm. The position of the three weld passes in the triple-pass weldment, which is of the same dimensions, and their order with respect to the x axis filling the groove, are shown in Fig. 3b, their centres are at x = +6.6 mm, 0 mm, and −6.6 mm.

3. The neutron diffraction measurements

The neutron diffraction method of residual stress measurement [5] is based on measurement of the lattice strain, averaged over a gauge volume in the sample. The difference in lattice spacing, d, determined from the Bragg angle of diffraction from the gauge volume, relative to that, d_0, from a reference strain-free sample is used to calculate strain Σ as:

$$\sum = (d - d_0)/d_0$$

The measurements were made on the SALSA instrument at the Institute Laue Langevin, Grenoble [7]. This instrument is situated on a thermal guide which transports the neutrons from the reactor onto a bent silicon monochromator. The angle of the diffracted beam from the monochromator is defined by a soller slit collimator. This defines the wavelength of the incident beam on the sample, and the beam area is defined by a slit aperture. The diffracted beam from the sample is defined by a slit aperture close to the sample and a two-dimensional (2D) position-sensitive detector. This slit aperture and detector can be rotated about the sample table axis to define the angle, 2θ, of the diffracted beam relative to the incident beam. The two slit apertures can be adjusted in position relative to the sample along the incident and diffracted beam directions, and their size defines the size of the instrumental gauge volume, over